Satellites to Seafloor

TOWARD FULLY AUTONOMOUS OCEAN SAMPLING

By Andrew F. Thompson, Yi Chao, Steve Chien, James Kinsey, M. Mar Flexas, Zachary K. Erickson, John Farrara,
David Fratantoni, Andrew Branch, Selina Chu, Martina Troesch, Brian Claus, and James Kepper

ABSTRACT. Future ocean observing systems will rely heavily on autonomous vehicles to achieve the persistent and heterogeneous measurements needed to understand the ocean's impact on the climate system. The day-to-day maintenance of these arrays will become increasingly challenging if significant human resources, such as manual piloting, are required. For this reason, techniques need to be developed that permit autonomous determination of sampling directives based on science goals and responses to in situ, remote-sensing, and model-derived information. Techniques that can accommodate large arrays of assets and permit sustained observations of rapidly evolving ocean properties are especially needed for capturing interactions between physical circulation and biogeochemical cycling. Here we document the first field program of the Satellites to Seafloor project, designed to enable a closed loop of numerical model prediction, vehicle path-planning, in situ path implementation, data collection, and data assimilation for future model predictions. We present results from the first of two field programs carried out in Monterey Bay, California, over a period of three months in 2016. While relatively modest in scope, this approach provides a step toward an observing array that makes use of multiple information streams to update and improve sampling strategies without human intervention.

SCIENTIFIC AND TECHNICAL MOTIVATION

A fundamental problem in oceanography is that key processes span many orders of magnitude in spatial and temporal scales. For instance, the global overturning circulation, occurring on scales of $O(10^8$ m, 10^{10} s), is tightly coupled to water mass modification that occurs on scales of $O(10^{-2}$ m, 1 s)—a variation of 10 orders of magnitude in both space and time. Ocean observational strategies have typically been focused on capturing a specific part of this range; for example, mooring arrays and the Argo network of autonomous profiling floats cover large temporal and spatial scales,

respectively, while scientific cruises that collect water samples or deploy high-resolution (e.g., microstructure) profilers may resolve the very smallest scales. Observational strategies are moving toward increasing the range of measured scales through the use of remote sensing, high-frequency radar, Lagrangian instruments, and other techniques.

Many key research questions related to the ocean's role in the climate system lie at the interface of traditional oceanographic disciplines. An interdisciplinary approach is needed that prioritizes scales where ocean physics, chemistry, and biology are most strongly coupled. Recent work shows that many essential processes,

such as air-sea fluxes, nutrient transport, and water mass subduction, occur at the ocean submesoscale (Lévy et al., 2012; Mahadevan, 2016). At the submesoscale, ocean dynamics evolve on time scales of days and over length scales between 1 km and 20 km, ranges that are difficult to capture observationally. Furthermore, moving beyond local process studies, measuring the impact of submesoscale motions and ocean properties on larger scales, or globally, will require an intelligent allocation of finite resources. Finally, the need to collect coincident information about physical, chemical, and biological variables requires sampling with a broad range of sensors that typically cannot be accommodated on a single platform.

Distributions of physical and biogeochemical properties (e.g., temperature, primary productivity) in the ocean are patchy (Martin et al., 2002). This is particularly acute in the upper ocean at spatial scales between 10 km and 50 km and over time scales of 24 hours to a few days. Fluid motions at these scales, typically referred to as the mesoscale, have a strong influence on planktonic community structure in the upper ocean and at upper trophic levels (Lévy et al., 2013; Siegel et al., 2016). Submesoscale motions also generate strong vertical velocities that may contribute significantly to the total export of carbon from the surface ocean into the interior ocean (Omand et al., 2015). Thus,

the marine carbon cycle responds dramatically to individual events that are spatially and temporally intermittent. A striking example is annual spring blooms: in a period of a few days, an intricate balance between surface heating, vertical nutrient fluxes, and upper ocean turbulence triggers rapid growth in phytoplankton that completely restructures carbon and nutrient concentrations and fluxes in localized ocean regions (Sverdrup, 1953; Mahadevan et al., 2012). This intermittency makes it difficult to identify and study the evolution of surface dynamics from a static array of assets. Scaling this regional example up to a global physical-biological observing array would require a large number of platforms in different regions that may be targeting different scales and different physical dynamics.

In 2013–2014, the Keck Institute for Space Studies (KISS) conducted a six-month study to investigate the premise that autonomous, coordinated groups of ocean robots programmed to use remote-sensing information and shore-based data assimilation could significantly advance our ability to obtain ocean observations needed to constrain the marine carbon cycle (Figure 1; A. Thompson et al., 2015). The primary conclusion of this study was *the need to develop techniques that allow heterogeneous groups of robots to autonomously determine sampling strategies with the help of numerical ocean forecasts and remotely sensed observations*. This work builds on earlier coordinated efforts to optimize marine autonomous observing networks.

Previous attempts at designing ocean observing systems that use multiple vehicles were conducted either with extensive human interaction or non-adaptive sampling approaches. Major efforts that involved adaptive surveys with multiple gliders under various degrees of automated control include the Autonomous Ocean Sampling Networks (Curtin et al., 1993; F. Zhang et al., 2007; Curtin and Bellingham, 2009), the Adaptive Sampling and Prediction (ASAP; Leonard et al., 2010), and the Shallow Water 06 (SW06; Tang et al., 2007) programs. There have been several efforts to use high-resolution assimilating numerical ocean models for planning vehicle trajectories (e.g., Smith et al., 2010; D. Thompson et al., 2010; Wang et al., 2013). Finally, fleets of multiple heterogeneous ocean robots have been deployed for projects like REP (Rapid Environment Picture) and CANON (Controlled, Agile, and Novel Observing Network; Y. Zhang et al., 2012; Das et al., 2014). A companion article, Flexas et al. (in press), details feature-tracking activities associated with the current KISS field program.

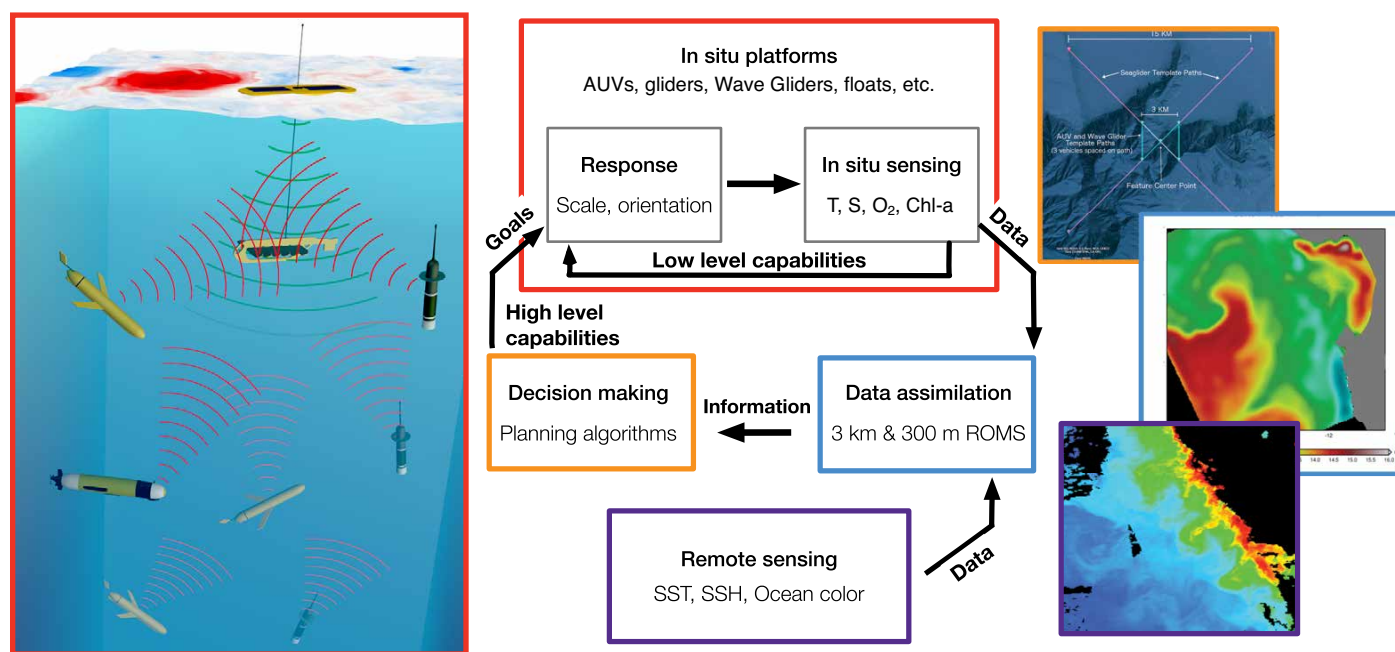Here we report on the first field season associated with the technical

FIGURE 1. Schematic and work flow of the Satellites to the Seafloor Keck Institute for Space Studies (KISS) concept (A. Thompson et al., 2015). The design calls for a combination of in situ (red) and satellite-based (purple) measurements to be assimilated into a high-resolution numerical model (blue). Both model output and observations are passed to a suite of planning algorithms (orange) that direct the in situ observing array, accounting for the varying capabilities and health of each instrument. Right-hand panels show an example of a path-planner template (orange), sea surface temperature in Monterey Bay from the 300 m resolution numerical output (blue, see Figure 2), and coastal California ocean color from the NASA Visible Infrared Imaging Radiometer Suite (VIIRS) scanning radiometer (purple).

development component of the KISS Satellites to Seafloor project, carried out in Monterey Bay between July and October 2016. The main goals of the field program were to (1) develop algorithms that maximize information gain from in situ observations with the use of shore-based circulation models; (2) design a framework in which a fleet of heterogeneous ocean robots can receive directives from shore-based models that consider the health, sensing, navigation, and communication characteristics of the robots; and (3) implement these methods on a range of vehicles, including autonomous underwater vehicles (AUVs), underwater gliders, and autonomous surface vehicles (ASVs). Considering the need for future ocean observing systems with longer persistence and increased asset heterogeneity and complexity, human control and

piloting of the array is unlikely to be feasible. For this reason, a guiding principle of this project is to develop scalable techniques that can accommodate large arrays of assets and permit sustained observations of the upper ocean's rapidly evolving submesoscale.

PROJECT COMPONENTS

The KISS field program was comprised of three components: (1) a numerical modeling effort to forecast the evolution of mesoscale and submesoscale structure, (2) a suite of algorithms to autonomously identify submesoscale features and to determine optimal sampling patterns, and (3) an array of in situ assets to implement the planned sampling pattern. The field program was conducted in multiple stages that focused on different spatial scales and sampling strategies.

Regional Ocean Modeling System (ROMS)

During the KISS field experiment, a nested ROMS-based coastal ocean modeling and data assimilation system provided both nowcast and forecast on a daily basis. ROMS is an open-source model developed by the oceanographic community (Shchepetkin and McWilliams, 2005). In the configuration used here, the innermost ROMS domain covers the greater Monterey Bay region to about 75 km offshore with a horizontal resolution of approximately 300 m. It is nested within an intermediate ROMS domain with a horizontal resolution of 1.1 km covering the coast from Pt. Reyes to Morro Bay and out to about 250 km offshore. The outermost ROMS domain covers the entire California coastal ocean from north of Crescent City, California, to Ensenada, Mexico, with a resolution of 3.3 km (Figure 2). In the vertical, there are 40 unevenly spaced sigma levels—a type of terrain-following vertical coordinate—used in all three ROMS domains, with the majority of these clustered near the surface to better resolve near-surface processes.

Tidal forcing is added through lateral boundary conditions that are obtained from a global barotropic tidal model (TPXO.6; Egbert et al., 1994; Egbert and Erofeeva, 2002). Lateral boundary conditions for the California domain are derived from global HYCOM (Hybrid Coordinate Ocean Model) forecasts (http://hycom.org). Both boundary conditions are provided at the outermost 3.3 km ROMS domain. The atmospheric forcing required by the ROMS model is derived from hourly operational forecast output performed with the NCEP (National Center for Environmental Prediction) 5 km North American model (NAM). An essential component of the nowcast and forecast system is the data assimilation scheme, a mathematical methodology for optimally synthesizing different types of observations with model first guesses (that is, forecasts). A new two-step multiscale (MS)
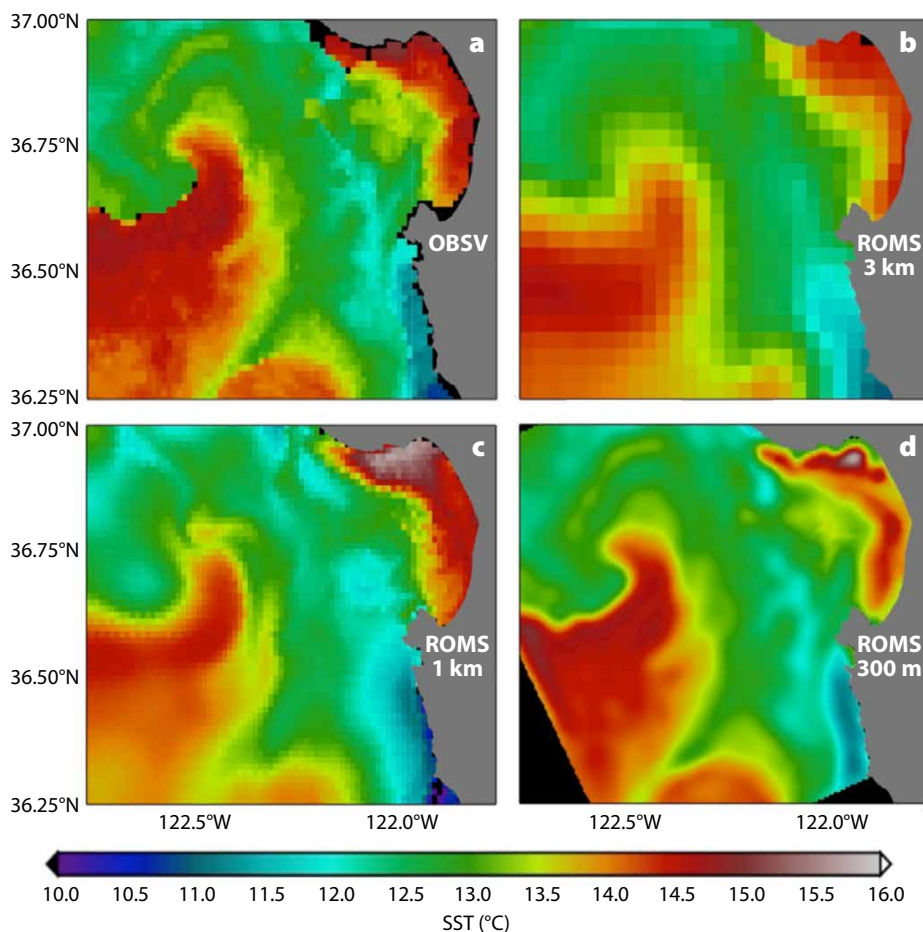

FIGURE 2. Sea surface temperature (°C) for April 5, 2016, (a) as observed by AVHRR/MODIS satellites, and as simulated in the three nested Regional Ocean Modeling System (ROMS) domains: (b) California 3 km, (c) central California 1 km, and (d) Monterey Bay 300 m. See text for further discussion.

three-dimensional variational (3DVAR) data assimilation algorithm is used here. This MS-3DVAR scheme is a generalization of the 3DVAR methodology of Li et al. (2008) and is described in detail in Li et al. (2015). The MS-3DVAR data assimilation methodology was selected because of its ability to propagate observational information, which is often sporadically and irregularly distributed in both the horizontal and vertical directions through an advanced error covariance formulation, as well as its computational efficiency that enables real-time operational forecasting.

The ROMS nowcast/forecast system is run daily in near-real time. The system incorporates all available real-time streams of data gathered from in situ or remote platforms, and is executed following the procedures of numerical weather prediction at operational meteorological centers. An assimilation step is carried out every six hours. The near-real time operation schedule during the KISS field experiment was designed to minimize the time lag between nowcast and forecast model times and real time and to ensure that the 48-hour model forecast was available by 5:00 am local time (PDT). More details on our modeling system, including the data assimilation methodology and a validation of the operational results, can be found in Chao et al. (2017).

As an example of the significant impact that increased horizontal resolution can have on the fidelity of the representation of small-scale features in the model fields, Figure 2 shows the daily mean sea surface temperature (SST) on April 5, 2016, as observed by AVHRR/MODIS (Advanced Very High Resolution Radiometer/Moderate-resolution Imaging Spectroradiometer), as well as the daily output of the model nowcasts with increasing resolutions from 3 km to 1 km and 300 m. On this particular day, a large standing mesoscale eddy is observed off the continental shelf. This feature is associated with warmer SSTs and separated from warmer

coastal water by a band of lower SST related to a wind-driven upwelling front (Ryan et al., 2005). Submesoscale features associated with small-scale eddies and filaments that are not well simulated by the relatively coarser models at 3 km and 1 km resolutions are reproduced by the model at 300 m resolution, for example, a filament of warmer SST located at 36.9°N and 122.5°W. Furthermore, the lateral scales and intensity of the cooler upwelled waters are more accurately captured in the 300 m ROMS model.

Feature Detection and Path Planning

The KISS observing system relies on a suite of feature detection algorithms, applied to the ROMS model output, to identify "target" locations for the in situ assets. Targets are defined by persistent (identified over a period of a day or longer) submesoscale physical oceanographic structures. With an appropriate sensor payload, the sampling strategies described herein are equally applicable to features defined by biological and/or chemical signatures. During the field program, a range of different upper ocean diagnostics were considered, including surface vorticity, lateral buoyancy gradients, and surface speed. Ultimately, we used horizontal SST gradients to detect surface fronts. The planning algorithm not only identified regions of enhanced SST gradients but also tracked the evolution of these features over multiple days using the gridded, three-dimensional, time-dependent ROMS ocean model with a time step of one hour.

The feature detection algorithm utilizes the two-dimensional spatial layout of SST at each time step t_i. Features are selected based on the gradient of the smoothed SST ($|\nabla SST|$) data using the Savitzky-Golay filter (Savitzky and Golay, 1964), a low-pass filter with a moving window. The feature detection algorithm chooses N features with the highest gradients at time t_0. To alleviate the problems of rapid merging of initial high-gradient regions, the entire grid

is initially subdivided into equal sections and a target is selected from each section. Each feature is tracked in time by estimating the projected trajectory, including a user-defined velocity constraint that restricts the distance traveled between successive t_i. In this approach, nearby features are allowed to merge during the tracking procedure.

The path planner produces control directives that instruct the assets to follow a template path relative to the identified feature. Two different template paths were developed: straight transects for the slower instrumentation, such as gliders, and bowtie shapes for the faster AUV assets. Future iterations could also optimize the sampling template. The path planner simulates the movement of an asset through the ocean using a movement model that dictates the undulation of the vehicle at a glide slope to the designated depth applying the control directive and the interpolated ROMS current velocity at the relevant latitude, longitude, depth, and time.

For each communication between shore and vehicle, a new plan is generated, covering multiple dives in case of poor communications. The template path (transect, bowtie) indicates a target latitude and longitude for the next vehicle surfacing. The planner considers a range of heading control directives and selects the control directive that, when simulated, minimizes error between the simulated surfacing location and the target location. This process is repeated until a set time period is reached.

Critically, the same planning algorithm accommodates assets with different characteristics. For our Monterey study, we used ocean gliders and AUVs. Despite the differences in vehicle characteristics (AUVs are much faster, gliders dive much deeper), the same planning algorithm was used for both types of vehicles. Glider plans are regenerated at each surfacing. For the AUVs, plans were generated daily for both moving and stationary features and were provided to the AUV operational team for deployment.

Glider and AUV Operations

Two different classes of autonomous vehicles were deployed during this field program: underwater gliders and propelled AUVs. The long-term gliders, one Seaglider (SG621) and one Spray glider (NPS34), were deployed in July 2016 to provide an overview of the hydrographic and biogeochemical properties of the study area. The gliders were piloted to sample perpendicular to the continental slope, which hosts a series of frontal currents, in particular at the shelf break (Figure 3a; Ryan et al., 2005; Flexas et al., in press). The gliders were flown in parallel sections with a lateral separation of ~20 km to permit calculation of lateral gradients at the submesoscale; for larger numbers of vehicles, the optimal separation between assets would also be determined by the planner. Due to the relatively shallow depths over the continental shelf and the gliders' slow speeds, the gliders did not sample in depths less than ~150 m. Unfortunately, due to inclement weather conditions during the field program, it was not possible to carry out spatially co-located deployments of the gliders and the AUVs. Therefore, the path planning efforts focused on the AUV sampling, while the gliders were used to carry out autonomous feature-tracking activities, as described in a later section on Deep Fronts and Feature Tracking.

The paths generated using the ROMS model were applied during an intensive AUV field program that was supported by R/V *Shana Rae* operating out of Santa Cruz, California. A typical operational cycle was to leave dockside at 5:00 am local time, with the AUVs fully charged and missions loaded, steam to targeted feature locations, deploy vehicles, monitor their progress, and recover early afternoon. A steaming time of about two to three hours from Santa Cruz to targets enabled us to capture a selection of features.

The observing platforms used for this field experiment consisted of three Iver2 (Ocean Server Technology Inc.) AUVs. All three of the vehicles were equipped with a 25 kHz Woods Hole Oceanographic Institution acoustic micro-modem and a hull-mounted Neil Brown conductivity/temperature sensor (Ocean Sensors Inc.). Additionally, two vehicles were configured with the YSI 6-Series Multiparameter Water Quality Sonde for sensing various biochemical parameters. All three vehicles operated at the most energy efficient speed of 2.5 knots and endured mission lengths of approximately 3.5 hours while expending less than 60% of total battery capacity. All three vehicles conducted undulating dives to depths of 20 m, 40 m, 60 m, and 80 m in a bow-tie type trajectory over a 3 km² area. Figure 4 displays an example of trajectory and temperature data gathered by the AUVs on September 2, 2016. We acknowledge that the 3.5-hour deployment durations mean that for this field program the primary goal was feature detection; future deployments would use similar techniques to capture feature evolution.

The field program schedule provided one week to implement and verify the overall KISS project concept. The week was divided between software and hardware testing, proofs of concepts, algorithm refinement, and finally, a full demonstration of the "start-to-finish" KISS project concept.

WIND-DRIVEN UPWELLING FRONTS

From August 27 to September 3, 2016, multiple deployments of the Iver2 AUVs were carried out over the continental shelf (Figure 3b). Each morning, the survey location was determined autonomously following analysis of the output from the ROMS 72-hour forecast arriving at 5:00 am. Due to the nearshore limitations of the sampling activities, we targeted
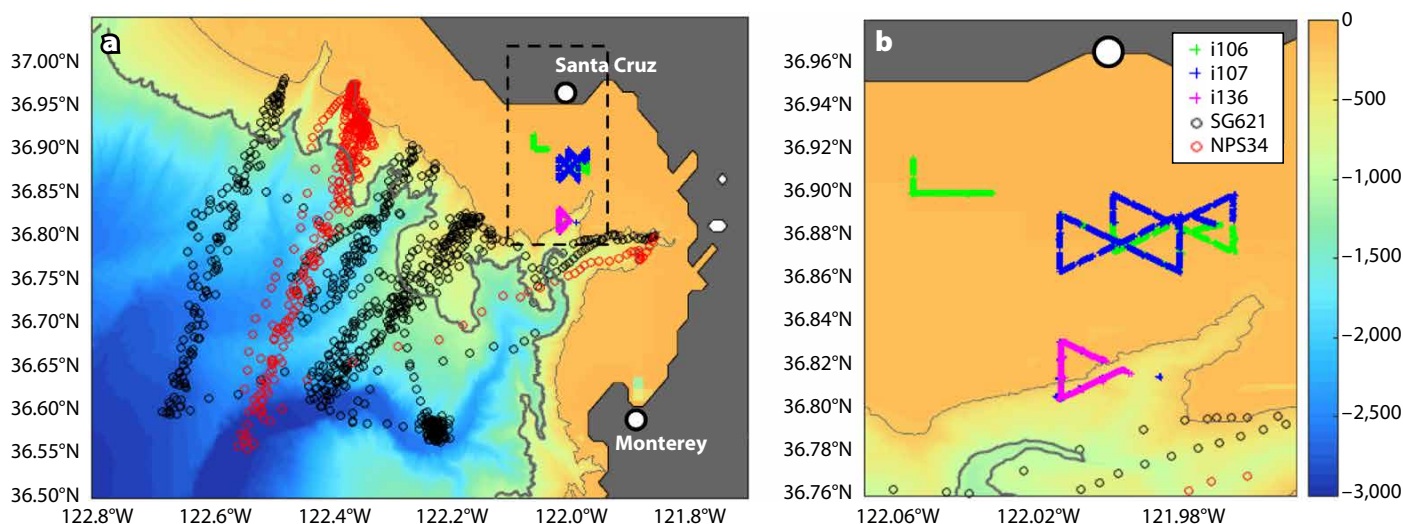

FIGURE 3. (a) Locations of all profiles carried out during the KISS field program in Monterey Bay between July and October 2016. Each symbol indicates a different asset, summarized in the legend in (b): gliders (SG621, NPS34) and Iver-class AUVs (i106, i107, i136). The region of intensive AUV deployments over the continental shelf is expanded in (b). Measurements collected in (b) occurred between August 27 and September 3. In both (a) and (b), the bathymetry (m) is given by the color; the 200 m and 1,000 m isobaths are contoured.

shallow upwelling fronts that are typically less than 10 km in scale. The full implementation of the KISS project concept was carried out on both the September 1 and 2; these dates correspond to the blue butterfly locations in Figure 3b.

An example of the implementation from September 2, 2016, is summarized in Figure 4. Panels (a) and (b) show snapshots of SST and the gradient of SST from the ROMS model corresponding to the expected deployment time of the assets (8:00 am local time). The autonomous feature detection accurately captured the strong temperature front (approximately 1°C km^{-1} and mapped out a butterfly pattern shown in white in these panels. As shown in panels (c) and (d), two AUVs (i106 and i107) were deployed just before

8:00 am and carried out the sampling pattern for a period of approximately four hours. The vertical structure of the temperature shown in panel (c) indicates that mixed layers were very shallow, ~20 m. However, even over this small domain, the AUVs were able to capture significant lateral temperature gradients. The yellow triangle in panel (d) highlights a period of reduced near-surface temperature, with temperature changing just over 1°C. This temperature difference is nearly half of the temperature drop across the front shown in panels (a) and (b). This feature is persistent over a period of 30 minutes, suggesting that it is not the signature of internal waves. The reduced surface temperature is also apparent as the glider returns to the western side of the butterfly

at the end of its sampling pattern.

The frontal structure captured by the AUV registered a 1°C temperature anomaly over a distance of ~1 km. This is equivalent to a lateral buoyancy gradient of 10^{-5} s^{-2}, which is indicative of a strong submesoscale front. Although the front was not located at the center of the sampling array, the fidelity between the model output and the observations is verified by capturing a front in this small (approximately 4 km × 4 km) domain. A limitation of this concept demonstration is the relatively short duration of the AUV deployment. This curtailed our ability to track the evolution of the front in time in order to determine both the fidelity of the numerical model over longer periods of time and the ability of the path
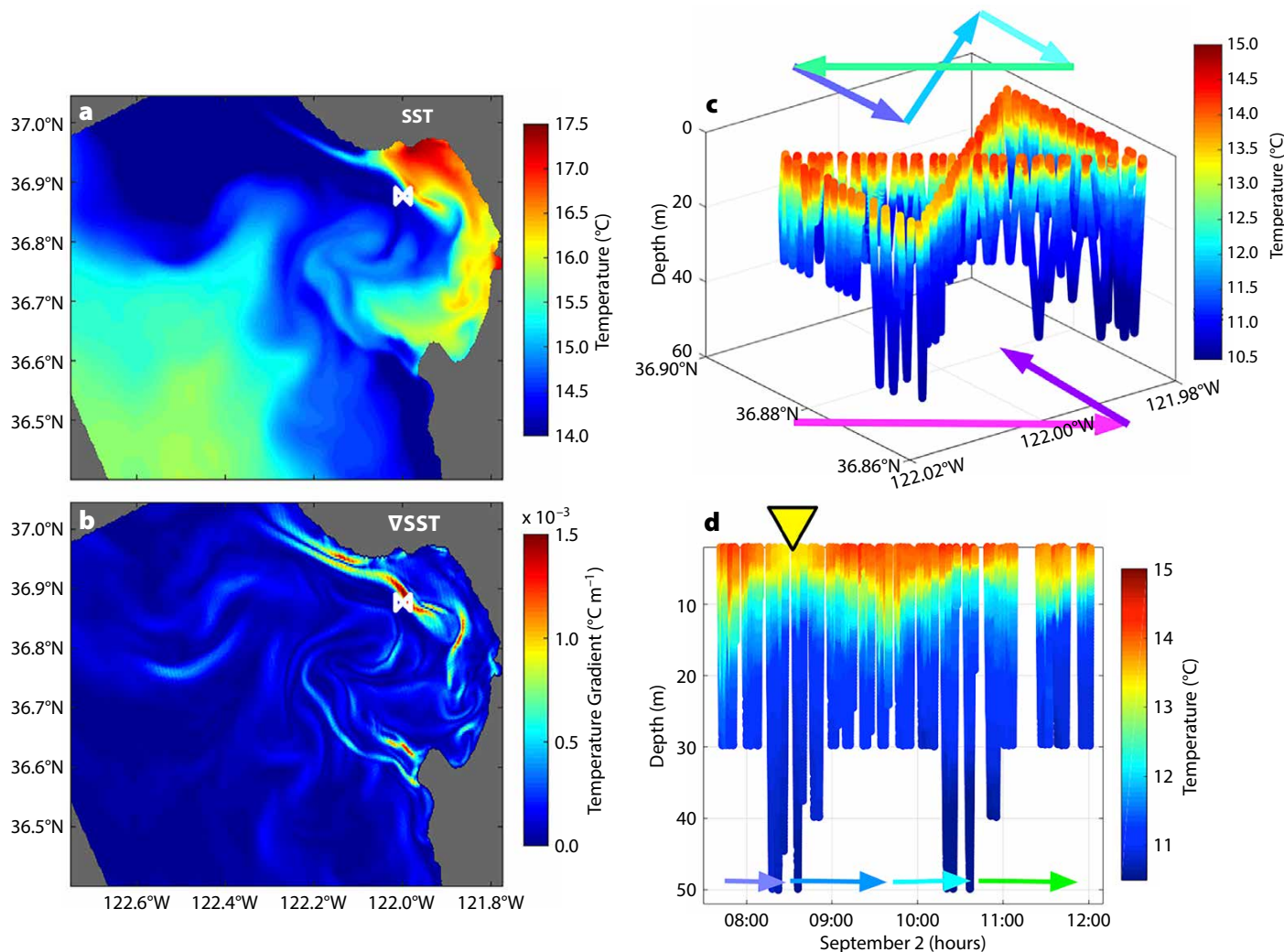

FIGURE 4. (a) Sea surface temperature (°C) and (b) sea surface temperature gradient (°C m^{-1}) from the 300 m ROMS model output on September 2, 2016, at 8:00 am local time (1500 UTC). In each panel, the white butterfly pattern indicates the sampling position determined by the planner. (c) Temperature and position of two Iver vehicles (i107, upper arrows; i106, lower arrows) on September 2, 2016. (d) Temperature time series from Iver vehicle i107. The colored arrows correspond to the legs of the butterfly, as shown in panel (c). The position of the upwelling front is indicated by the yellow triangle.

planner to follow the movement of the front. In future iterations, a combination of model output and in situ observations will be used to update the sampling patterns (Figure 1).

DEEP FRONTS AND FEATURE TRACKING

In addition to the near real-time experiments carried out over the continental shelf, we also explored autonomous methods for detecting submesoscale fronts and optimizing sampling of these features without human intervention. This approach uses 48-hour forecasts from the ROMS model described earlier, feature-tracking techniques, and an autonomous planner that controls the observing platform. This component

of the field program was carried out in October 2016.

Our targeted "features" for this activity are thermohaline structures, subducting from below the mixed layer into the deep ocean. Because these features are strongly density-compensated (they form along density surfaces, but are associated with large, compensated temperature and salinity gradients), we elect to diagnose spice π, as introduced by Flament (1986). The absolute value of spice is less important than spice variance, indicative of large variations in warm/salty and cold/fresh water masses along a density surface. Thus, the autonomous planner uses lateral, or along-track, gradients in spice, $\partial\pi/\partial x$, to detect features of interest. Spiciness has been widely used to study

the California Current System (Flament, 2002, and references therein). Isobaric and isopycnal hydrographic variability specifically from ocean gliders is characterized by Rudnick and Cole (2011) and Cole and Rudnick (2012).

Flexas et al. (in press) presents a detailed description of our feature-tracking activities, and they are briefly summarized here. Using the ROMS forecast, a series of simulated transects are determined along a track, nominally perpendicular to the continental slope (Figure 5a). For a given period, the simulated glider track can either continue straight or can be directed to "turn back" if a front is detected. Turning back on the front permits multiple realizations of the high-gradient region over a short period
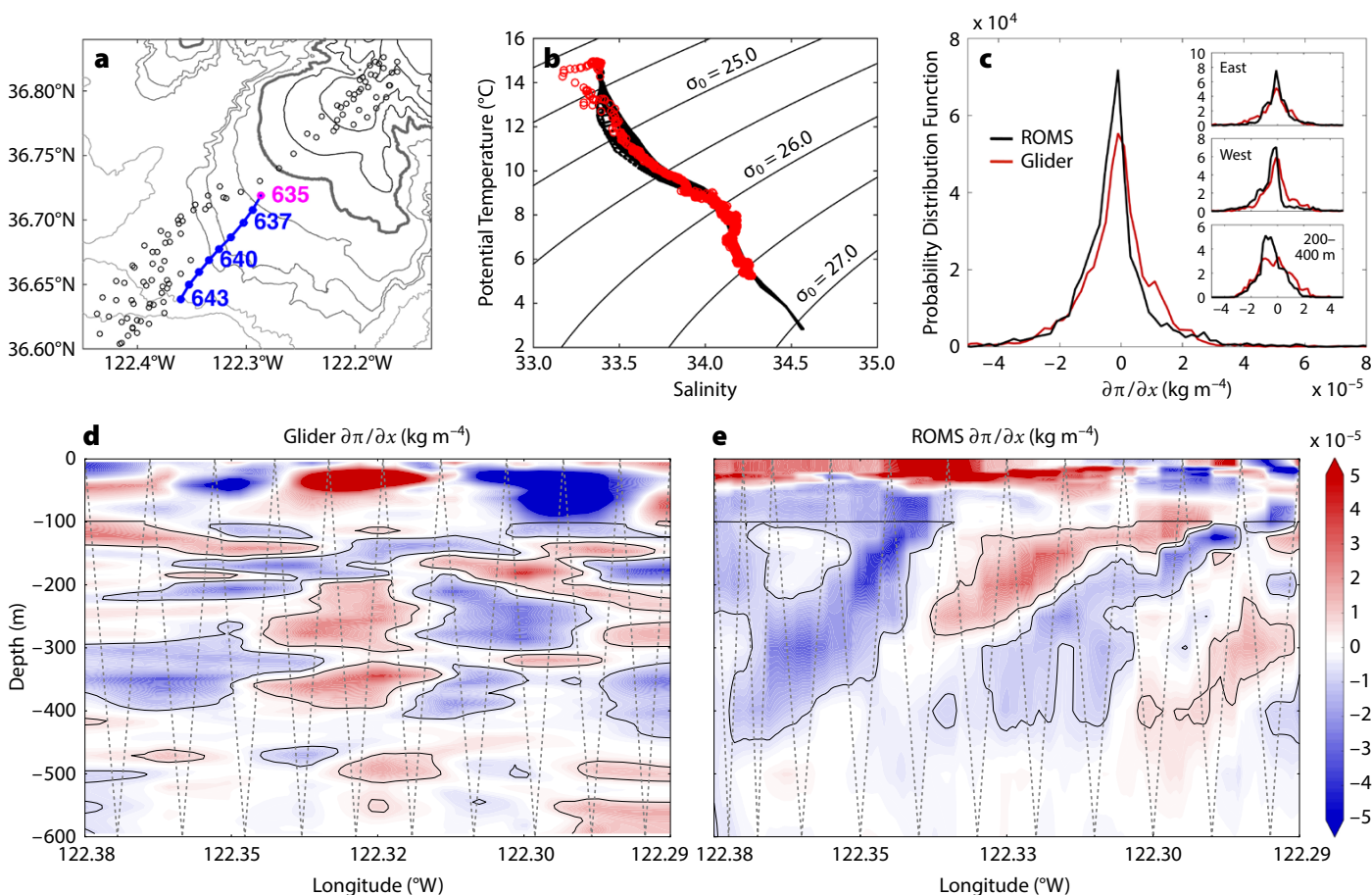

FIGURE 5. Feature-tracking experiment on October 22, 2016. (a) Glider path: black circles indicate all dives performed during the feature tracking experiment (October 22–30, 2016). Dives performed by the Seaglider (SG621) on October 22 are highlighted in blue (first dive, 635, is highlighted in magenta). The black contours show bathymetry at 200 m intervals; the 1,000 m isobath is shown in bold. (b) Temperature-salinity plot for the points extracted from the ROMS model (black) and from the glider data along the blue curve in panel (a) (red points). (c) Probability distribution function (PDF) of the lateral gradient of spice ($\partial\pi/\partial x$, kg m^{-4}) obtained from the glider (red) and shown in (d) and extracted from ROMS 300 m forecast output at glider locations (black) and shown in (e). Sub-panels show the PDF for the eastern and western halves of the sections as well as just between 200 m and 400 m. In the lower panels, black dotted lines indicate the position of the actual (d) and simulated (e) glider. Analysis of additional sections is shown in Flexas et al. (in press).

of time. The track selected is the one that optimally crosses the strongest lateral spice gradients. This track is then autonomously delivered to the glider as a series of way points.

Figure 5d shows an example of the lateral spice gradient observed from glider data on October 22, 2016. The ROMS-derived lateral spice gradient at the corresponding glider location is shown in panel (e) for comparison. Similar to the upwelling fronts described earlier, the location of the submesoscale fronts are not found at precisely the same location, but the vertical structure and magnitude of the variability is similar. We verify this by plotting a histogram of $\partial \pi / \partial x$ in panel (c), both for the entire transect and for subdomains of the transect. The distribution is similar, although ROMS tends to underestimate the gradients. Flexas et al. (in press) provide an analysis of multiple sections that suggest that the ROMS model is accurately capturing the physical process related to the subducting fronts and has skill in directing the glider(s) to a region of strong frontogenesis.

Based on model estimations, the sampling "gain," defined as the amount of spiciness gradient sampled, is 50% larger for gliders that are autonomously piloted by the feature-tracking planner as compared to a sampling pattern that simply samples across the entire width of the continental slope (Flexas et al., in press).

PERSPECTIVES

Future ocean observing arrays will inevitably move toward greater levels of autonomy using larger fleets of a given platform or with arrays of heterogeneous assets. This project builds upon previous and ongoing efforts that have appreciated the need for adaptable observing arrays but that have typically involved intensive human interpretation of the information being returned by the vehicles in real time. We argue that this level of human involvement is not sustainable because (a) it becomes difficult to maintain persistent observations in this mode,

and (b) the quantity of data generated by models and satellites (and potentially multiple in situ instruments) makes it too difficult to carry out near-real-time synthesis. As the need to acquire information that crosses traditional biological/chemical/physical disciplines increases, the burden on human resources will also increase. A solution is to cede more control over lower-level tasks, such as target determination and sampling strategies, to the vehicles and planning software (Figure 1).

In this study and during our first field program, we laid out a framework for ocean sampling with limited human intervention. Successes of the mission include substantial evidence that near-real-time data assimilation of both in situ and remote-sensing information in a high-resolution numerical model can improve the targeting of coherent structures on the time scale of a day. Our feature-tracking component of the field experiment also showed that an autonomous dive-by-dive assessment of the frontal conditions can improve the efficiency of sampling with gliders. Up to 50% more time is spent sampling coherent frontal regions. Finally, we showed that by assimilating the in situ data into the ROMS model, the fidelity of the forecasts improved, suggesting a positive feedback between model reliability, improved target planning, and more beneficial observations for future assimilation. Achieving fully autonomous observational arrays requires further development and testing. For instance, during our field program we were unable to carry out a nested array incorporating assets with different characteristics (e.g., speed, sensor suite). Ideally, longer deployments would have allowed us to make a better assessment of how autonomous data acquisition improves our ability to capture the evolution of submesoscale structure in the ocean. This is the focus of our second field program, in 2017.

LeTraon (2013) argues that oceanography has undergone three major revolutions in the past three decades. The first

is related to the advent of satellite oceanography, which provided global synoptic information about ocean surface properties and variability. The second is related to the realization of the Argo float array, which benefited heavily from the advantages of autonomous sampling to achieve a global subsurface observing system. The third revolution is the implementation of global operational oceanography. Yet, these three aspects of observational oceanography are rarely used synergistically in real time. A primary goal of the KISS study is to effectively couple information from these different streams—achieving this with minimal, or low-level, human effort should aid in the synthesis of these diverse data sets. Key scientific questions that require an understanding of processes across multiple temporal and spatial scales, including the impact of submesoscale motions on the large-scale ocean circulation (McWilliams, 2016) and biogeochemical cycling (Lévy et al., 2012), are poised to take advantage of these new capabilities. 🔁

REFERENCES

Chao, Y., J.D. Farrara, H. Zhang, K.J. Armenta, L. Centurioni, F. Chavez, J.B. Girton, D. Rudnick, and R.K. Walker. 2017. Development, implementation, and validation of a California coastal ocean modeling, data assimilating and forecasting system. *Deep Sea Research Part II,* https://doi.org/10.1016/j.dsr2.2017.04.013.

Cole, S.T., and D.L. Rudnick. 2012. The spatial distribution and annual cycle of upper ocean thermohaline structure. *Journal of Geophysical Research* 117, C02027, https://doi.org/10.1029/2011JC007033.

Curtin, T.B., and J.G. Bellingham. 2009. Progress toward autonomous ocean sampling networks. *Deep Sea Research Part II* 56:62–67, https://doi.org/10.1016/j.dsr2.2008.09.005.

Curtin, T.B., J.G. Bellingham, J. Catipovic, and D. Webb. 1993. Autonomous oceanographic sampling networks. *Oceanography* 6(3):86–94, https://doi.org/10.5670/oceanog.1993.03.

Das, J., F. Py, T. Maughan, T. O'Reilly, M. Messie, J. Ryan, K. Rajan, and G. Sukhatme. 2014. Simultaneous tracking and sampling of dynamic oceanographic features with autonomous underwater vehicles and Lagrangian drifters. Pp. 541–555 in *Experimental Robotics*. Springer.

Egbert, G.D., A.F. Bennett, and M.G.G. Foreman. 1994. TOPEX/POSEIDON tides estimated using a global inverse model. *Journal of Geophysical Research* 99:24,821–24,852, https://doi.org/10.1029/94JC01894.

Egbert, G.D., and S.Y. Erofeeva. 2002. Efficient inverse modeling of barotropic ocean tides. *Journal of Atmospheric and Oceanic Technology* 19:183–204, https://doi.org/10.1175/1520-0426(2002)019<0183:EIMOBO>2.0.CO;2.

Flament, P. 1986. *Finestructure and Subduction Associated with Upwelling Filaments*. PhD Thesis, University of California, San Diego.

Flament, P. 2002. A state variable for characterizing water masses and their diffusive stability: Spiciness. *Progress in Oceanography* 54:493–501, https://doi.org/10.1016/S0079-6611(02)00065-4.

Flexas, M.M., M.I. Troesch, S. Chu, A. Branch, S. Chien, A.F. Thompson, J. Farrara, and Y. Chao. In press. Autonomous sampling of ocean submesoscale fronts with ocean gliders and numerical forecasting. *Journal of Atmospheric and Oceanic Technology*.

Leonard, N.E., D.A. Paley, R.E. Davis, D.M. Fratantoni, F. Lekien, and F. Zhang. 2010. Coordinated control of an underwater glider fleet in an adaptive ocean sampling field experiment in Monterey Bay. *Journal of Field Robotics* 27:718–740, https://doi.org/10.1002/rob.20366.

LeTraon, P.Y. 2013. From satellite altimetry to Argo and operational oceanography: Three revolutions in oceanography. *Ocean Science* 9:901–915, https://doi.org/10.5194/os-9-901-2013.

Lévy, M., L. Bopp, P. Karleskind, L. Resplandy, C. Ethe, and F. Pinsard. 2013. Physical pathways for carbon transfers between the surface mixed layer and the ocean interior. *Global Biogeochemical Cycles* 27:1,001–1,012, https://doi.org/10.1002/gbc.20092.

Lévy, M., R. Ferrari, P.J.S. Franks, A.P. Martin, and P. Rivière. 2012. Bringing physics to life at the submesoscale. *Geophysical Research Letters* 39, L14602, https://doi.org/10.1029/2012GL052756.

Li, Z., Y. Chao, J.C. McWilliams, and K. Ide. 2008. A three-dimensional variational data assimilation scheme for the Regional Ocean Modeling System. *Journal of Atmospheric and Oceanic Technology* 25:2,074–2,090, https://doi.org/10.1175/2008JTECHO594.1.

Li, Z., J.C. McWilliams, K. Ide, and J.D. Farrara. 2015. Coastal ocean data assimilation using a multiscale three-dimensional variational scheme. *Ocean Dynamics* 65:1,001–1,015, https://doi.org/10.1007/s10236-015-0850-x.

Mahadevan, A. 2016. The impact of submesoscale physics on primary productivity of plankton. *Annual Review of Marine Science* 8:161–184, https://doi.org/10.1146/annurev-marine-010814-015912.

Mahadevan, A., E.A. D'Asaro, C. Lee, and M.J. Perry. 2012. Eddy-driven stratification initiates North Atlantic spring phytoplankton blooms. *Science* 337:54–58, https://doi.org/10.1126/science.1218740.

Martin, A.P., K.J. Richards, A. Bracco, and A. Provenzale. 2002. Patchy productivity in the open ocean. *Global Biogeochemical Cycles* 16(2), https://doi.org/10.1029/2001GB001449.

McWilliams, J.C. 2016. Submesoscale currents in the ocean. *Proceedings of the Royal Society A* 472(2189), https://doi.org/10.1098/rspa.2016.0117.

Omand, M.M., E.A. D'Asaro, C.M. Lee, M.J. Perry, N. Briggs, I. Cetini, and A. Mahadevan. 2015. Eddy-driven subduction exports particulate organic carbon from the spring bloom. *Science* 348:222–223, https://doi.org/10.1126/science.1260062.

Rudnick, D.L., and S.T. Cole. 2011. On sampling the ocean using underwater gliders. *Journal of Geophysical Research* 116, C08010, https://doi.org/10.1029/2010JC006849.

Ryan, J.P., F.P. Chavez, and J.G. Bellingham. 2005. Physical-biological coupling in Monterey Bay, California: Topographic influences on phytoplankton ecology. *Marine Ecology Progress Series* 287:23–32, https://doi.org/10.3354/meps287023.

Savitzky, A., and M.J.E. Golay. 1964. Smoothing and differentiation of data by simplified least squares procedures. *Analytical Chemistry* 36:1,627–1,639, https://doi.org/10.1021/ac60214a047.

Shchepetkin, A.F., and J.C. McWilliams. 2005. The Regional Ocean Modeling System: A split-explicit, free-surface, topography-following-coordinate ocean model. *Ocean Modelling* 9:347–404, https://doi.org/10.1016/j.ocemod.2004.08.002.

Siegel, D.A., K.O. Busseler, M.J. Behrenfeld, C.R. Benitez-Nelson, E. Boss, M.A. Brzezinski, A. Burd, C.A. Carlson, E.A. D'Asaro, S.C. Doney, and others. 2016. Prediction of export and fate of global ocean net primary production: The EXPORTS science plan. *Frontiers in Marine Science* 3:22, https://doi.org/10.3389/fmars.2016.00022.

Smith, R.N., Y. Chao, P. Li, D.A. Caron, B.H. Jones, and G.S. Sukhatme. 2010. Planning and implementing trajectories for autonomous underwater vehicles to track evolving ocean processes based on predictions from a regional ocean model. *International Journal of Robotic Research* 29:1,475–1,497, https://doi.org/10.1177/0278364910377243.

Sverdrup, H. 1953. On conditions for the vernal blooming of phytoplankton. *ICES Journal of Marine Science* 18:287–295, https://doi.org/10.1093/icesjms/18.3.287.

Tang, D., J.N. Moum, J.F. Lynch, P. Abbot, R. Chapman, P.H. Dahl, T.F. Duda, G. Gawarkiewicz, S. Glenn, J.A. Goff, and others. 2007. Shallow Water '06: A joint acoustic propagation/nonlinear internal wave physics experiment. *Oceanography* 20(4):156–167, https://doi.org/10.5670/oceanog.2007.16.

Thompson, A.F., J.C. Kinsey, M. Coleman, and R. Castano. 2015. *Satellites to the Seafloor: Autonomous Science to Form a Breakthrough in Quantifying the Global Ocean Carbon Budget*. Technical report, Keck Institute for Space Studies, California Institute of Technology, Pasadena, CA.

Thompson, D.R., S. Chien, Y. Chao, P. Li, B. Cahill, J. Levin, O. Schofield, A. Balasuriya, S. Petillo, M. Arrott, and others. 2010. Spatiotemporal path planning in strong, dynamic, uncertain currents. Pp. 4,778–4,783 in *2010 IEEE International Conference on Robotics and Automation (ICRA)*. IEEE.

Wang, X., Y. Chao, D.R. Thompson, S.A. Chien, J. Farrara, P. Li, Q. Vu, H. Zhang, J.C. Levin, and A. Gangopadhyay. 2013. Multi-model ensemble forecasting and glider path planning in the Mid-Atlantic Bight. *Continental Shelf Research* 63:S223–S234, https://doi.org/10.1016/j.csr.2012.07.006.

Zhang, F., D.M. Fratantoni, D.A. Paley, N.E. Leonard, and J.M. Lund. 2007. Control of coordinated patterns for ocean sampling. *International Journal of Control* 80:1,186–1,199.

Zhang, Y., M.A. Godin, J.G. Bellingham, and J.P. Ryan. 2012. Using an autonomous underwater vehicle to track a coastal upwelling front. *IEEE Journal of Oceanic Engineering* 37:338–347, https://doi.org/10.1109/JOE.2012.2197272.

ACKNOWLEDGMENTS

AUTHORS

Andrew F. Thompson (andrewt@caltech.edu) is Assistant Professor, Environmental Science and Engineering, California Institute of Technology, Pasadena, CA, USA. **Yi Chao** is Principal Scientist, Remote Sensing Solutions, Monrovia, CA, USA, and Adjunct Professor, University of California, Los Angeles, CA, USA. **Steve Chien** is Technical Group Supervisor, Artificial Intelligence Group, Jet Propulsion Laboratory, California Institute of Technology, Pasadena, CA, USA. **James Kinsey** is Associate Scientist, Applied Ocean Physics & Engineering, Woods Hole Oceanographic Institution, Woods Hole, MA, USA. **M. Mar Flexas** is Senior Research Scientist, and **Zachary K. Erickson** is a graduate student, both in the Department of Environmental Science and Engineering, California Institute of Technology, Pasadena, CA, USA. **John Farrara** is Scientist and **David Fratantoni** is Principal Scientist, both at Remote Sensing Solutions, Monrovia, CA, USA. **Andrew Branch** is Data Scientist, **Selina Chu** is Researcher, and **Martina Troesch** is Engineering Applications Software Engineer, all at Jet Propulsion Laboratory, California Institute of Technology, Pasadena, CA, USA. **Brian Claus** is Postdoctoral Investigator, Woods Hole Oceanographic Institution, Woods Hole, MA, USA. **James Kepper** is a student in the MIT/WHOI Joint Program in Oceanography, Woods Hole Oceanographic Institution, Woods Hole, MA, USA.

ARTICLE CITATION